

Received 23 July 2023, accepted 13 September 2023, date of publication 15 September 2023,
date of current version 20 September 2023.

Digital Object Identifier 10.1109/ACCESS.2023.3316024

RESEARCH ARTICLE

A Novel Network Optimization Scheme Based on Anti-Flocking and Improved Nash Equilibrium Algorithm

TIANJUN WANG¹, SHUCHANG ZHANG², LISHAN LIU², DUANPO WU²,
XINYU JIN³, SHUWEI CEN⁴, AND BING FAN⁵

¹School of Electronics and Information Engineering, Hangzhou Dianzi University, Hangzhou 310018, China

²School of Communication Engineering, Hangzhou Dianzi University, Hangzhou 310018, China

³Department of Information Science and Electronic Engineering, Zhejiang University, Hangzhou 310027, China

⁴China Mobile Communications Group Zhejiang Company Ltd., Hangzhou Branch, Hangzhou 310006, China

⁵Service Center for Advanced Technology, Hangzhou Dianzi University, Hangzhou 310018, China

Corresponding authors: Duanpo Wu (wudianpo@hdu.edu.cn) and Bing Fan (fanbing@hdu.edu.cn)


This work was supported in part by the Ministry of Education-China Mobile Research Fund under Grant MCM20-2017-0107; in part by the National College Student's Innovation and Entrepreneurship Training Program under Grant 202110336030; and in part by the Open Project of Zhejiang Provincial Key Laboratory of Information Processing, Communication and Networking, Zhejiang, China.

ABSTRACT Unmanned Aerial Vehicle (UAV) has very wide application prospect in aiding terrestrial cellular network communication, but it remains a challenge to optimize UAV locations and maximize user service rate during deployment. In this paper, a novel network optimization scheme based on anti-flocking model and improved Nash Equilibrium (NE) algorithm is proposed by studying the problem of dynamic UAV deployment and backhaul transmission. Firstly, the UAV-adaptive algorithm based on gray wolf optimization (U-GWO) is used to predeploy UAVs with limited number of UAVs. Secondly, ground mobile users are tracked by building a UAV-based anti-flocking (U-AF) model. Then, during the tracking of ground users by UAV, an improved NE strategy is used to establish the backhaul transmission links between UAVs, ground BSs and other UAVs to ensure that deployed UAVs can maximize the service rate and effective backhaul transmission rate of ground users. Simulation results show that the average service rate of User Equipment (UE) with U-GWO algorithm is improved from 1 % to 5.77 % compared to other different swarm intelligence optimization algorithms. And the service rate obtained with U-AF algorithm is 43.2 % improved compared to the baseline scenario without U-AF algorithm. For UAV backhaul transmission link construction, the simulation results show that the proposed improved NE strategy improves the average effective backhaul transmission rate by 12 %, the minimum backhaul transmission rate by 84 % and the overall iteration number by 5 % on average compared to a pure NE strategy.

INDEX TERMS Anti-flocking, gray wolf optimization, Nash equilibrium, relay, unmanned aerial vehicles.

I. INTRODUCTION

In the near future, as 5G technology continues to advance, we can expect our daily lives to be enriched with high-speed data transmission, minimal latency, and a diverse range of communication options [1], [2]. At the same time, the huge demand for data traffic services to meet the

The associate editor coordinating the review of this manuscript and approving it for publication was Guillermo Valencia-Palomo .

proliferation of User Equipments (UEs) in hotspots and the mobility and uneven distribution of UEs in hotspots pose significant difficulties for UEs serving hotspots [3], [4]. Hotspots can be effectively relieved through the utilization of aerial base stations (BSs) in the form of Unmanned Aerial Vehicles (UAVs), which offer exceptional flexibility during deployment, affordability, and adaptable terrain coverage [5], [6]. The integration of UAVs featuring Air-to-Ground (A2G) and Air-to-Air (A2A) capabilities within backhaul

transmission systems is generating immense interest, owing to its potential to achieve optimal information transmission efficiency, minimal data loss, and low transmission delays.

A. RELATED WORKS

Considering that UAVs can act as mobile aerial BSs, the problem of maximizing the user coverage area by deploying a limited number of UAVs needs to be addressed [7], and thus the deployment of UAV mounted BS (UAV-BS) has been extensively studied by many scholars [8]. A large number of studies on maximizing user coverage area aim to obtain maximum UE coverage rate and optimal UAV flight altitude. Chen et al. [9] studied the maximum reliability that can be achieved by placing UAVs. They assessed various factors such as total power loss, overall outage, and bit error rate (BER) to evaluate reliability. Their research determined the optimal flight altitudes for UAVs under both static and dynamic conditions. Alzenad et al. [10] decomposed the UAV-BS 3D deployment problem into separate horizontal and vertical explorations by maximizing UE coverage with minimal transmission power and constructing the UAV-BS horizontal deployment as a circular placement and minimum closed loop model. Yanikomeroglu et al. [11] presented an equivalent quadratically constrained mixed-integer nonlinear optimisation problem based on a three-dimensional placement problem with the objective of maximising network revenue, and proposed a computationally efficient numerical solution for the problem. Lai et al. [12] proposed a density-aware placement algorithm by modeling the UAV-BS coverage problem for arbitrarily distributed UEs as a NP-complete problem to obtain UEs that maximize coverage under constraints. In studying the UAV coverage performance problem, Zhang et al. [13] gave a coverage model of UAV and used coverage rate as the problem description quantity and proposed a swarm intelligence optimization algorithm using Particle Swarm Optimization (PSO) to optimize UAV deployment to obtain the maximum coverage rate of UE. Chowdhury and De [14] proposed an improved Reverse Glowworm Swarm Optimization (RGSO) algorithm to avoid possible collisions in the motion path of UAVs in their study of the 3D path planning problem of UAVs. A hybrid algorithm based on Improved Manta Ray Foraging Optimization and Tabu Search (IMRFO-TS) algorithm was proposed by AIT SAADI et al. [15] to obtain the optimal deployment location of UAVs in the network to improve its convergence speed and explore the UAV search area efficiently when studying the problem of building multi-UAV networks in the context of smart cities.

After determining the maximum UE coverage, sending the data information of each UE back to the BS in time becomes a priority, while establishing a direct link between the UE and the BS, the power loss of the information is huge for UEs that are far away from the BS, and the signal strength received by the BS will be significantly weakened at this time [16], [17]. To solve such problems, the UAV is used as a relay

between the UE and the BS, and then an optimal backhaul transmission link is constructed from the UE to the UAV and from the UAV to the BS, thus improving the efficiency of information transmission [18]. Fu et al. [19] proposed a distributed User Cluster (UC) algorithm based on wireless channel quality to enhance the signal reception strength of BS by constructing the use of multiple UAVs as a relay between Internet of Things (IoT) devices and BS. Yang et al. [20] introduced the concept of line-of-sight (LoS) and non-line-of-sight (NLoS) transmission of information links using UAVs as relays to provide data to Ground Robot (GR) with remote BSs and compared it with existing studies that ignored the effect of obstacles or assumed uniform obstacle distribution. The A2G Network Formation (A2G-NF) algorithm and the Communication Quality-aware UAV Placement (CQA-UP) algorithm were proposed to optimize the transmission of the A2G network by considering randomly distributed obstacles in the urban environment, in contrast to existing studies that ignore the effect of obstacles or assume a uniform distribution of obstacles. These algorithms can optimize the UAV multi-hop network to increase the amount of transmitted data and reduce transmission delay.

Recently, with some scholars considering the link composition among UAVs under the determination of UE maximization coverage, i.e., the dynamic composition of links when UAVs obtain optimal deployment, model construction for this type of problem needs to take into account the efficiency of UAV deployment and the transmission benefits of the constructed backhaul links, the temporal sequencing of UAVs for mobile deployment and link formation actions. Li et al. [21] proposed a flipping ambiguity avoidance optimization algorithm with gray wolf optimization (GWO) to improve the positioning accuracy in the UAV positioning problem. Lyu et al. [22] introduced a spiral placement algorithm for UAV deployment that reduces the number of Mobile Base Stations (MBS) needed to provide wireless coverage to distributed Ground Terminals (GTs) ensuring that every GT is within range of at least one MBS, with the MBS starting from the perimeter of the area containing uncovered GTs and following a spiral path to the center until all GTs are covered, achieving an optimal number of deployed UAVs while maintaining overall user coverage. Shi et al. [23] studied the path and deployment problems of UAV movement, and proposed an adaptive multi-UAV path planning method based on the GWO in response to the slow convergence speed and insufficient flight paths in path planning.

B. MOTIVATION AND CONTRIBUTIONS

This paper investigates the network coverage of mobile UEs and the composition of a multi-hop backhaul transmission link between UAVs and multiple BSs in real time. Since the context of the study is for hotspots, where there is huge connection pressure and excessive channel loss in BS, direct connection between UE and BS is not considered here.

A UAV-based anti-flocking (U-AF) algorithm is proposed for UAV access deployment¹ in a predefined context, where UE communication quality, UAV bearer capacity and service range are guaranteed. At the same time, an improved Nash Equilibrium (NE) strategy [24] is used to construct multi-hop backhaul links. To promote optimal NE balance both internally and externally, the randomized gaming process of a pure NE strategy has been replaced with a prioritized scheme in which UAVs positioned farthest from the BS are given preference to participate in the NE process, while efforts are made to minimize link loss related to UAVs not participating in the linked construction process. This scheme solves the UAV backhaul problem with a better layout for backhaul links. Our algorithm² consists of three stages. In the first stage, a UAV-adaptive gray wolf optimization (U-GWO) algorithm is designed. The U-GWO algorithm can output a better set of results in the multi-UAV deployment problem for UAV predeployment. In the second stage, an improved UE-based anti-flocking model will be designed to capture hotspot UEs, provide continuous hotspot area services, and avoid adverse effects such as possible collisions and interference caused by the proximity of UAVs during UAV deployment [25]. In the third stage, an A2G channel link preprocessing operation has been incorporated when it is discovered that, in the pure NE strategy, using a utility function may impede its effectiveness. The UAVs have been split into two categories: resident and nonresident. The former will not involved in the NE process for backhaul channel alteration. In conclusion, this paper makes the following primary contributions:

- 1) The U-GWO-based predeployment algorithm has been formulated and tested, producing an output of viable deployment locations based on iterative optimization. The numerical result is the most comprehensive coverage across UE service areas that can be achieved with a finite number of UAVs.
- 2) The U-AF can be designed to convert the UE's movement trend, the distance between UE and UAV, and the distance between the different UAVs into corresponding strategy effect. With this algorithm, the UAV can be guided to perform the corresponding movements and provide continuous and effective services to UE, and independently track UEs to determine their optimal locations.
- 3) The pure NE strategy is improved to achieve both internal and external layer equilibrium by introducing

¹The problem studied here is in continuous space, not in discrete space, where the probability of overlapping UAV positions is almost zero. In UAV pre-deployment, if the UAVs appear in the same location at this time, it will lead to a reduction in the number of UEs covered by the UAVs, which in turn will reduce the service rate of the UAVs, and this is something we need to avoid as much as possible.

²In the context of our setting, we will set up computationally powerful servers as clouds, which can be local BSs, and use each UAV as an edge-side device. And we will process complex data calculations that would otherwise require UAV processing through the cloud.

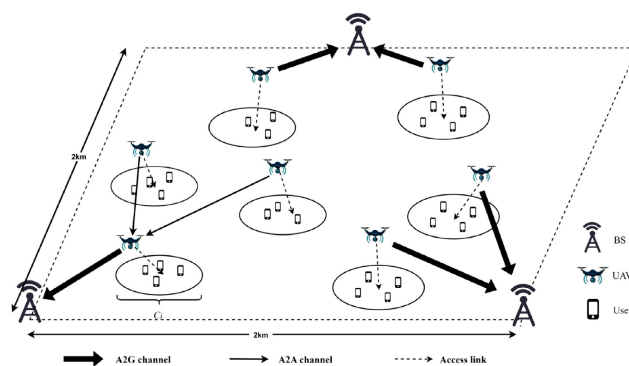


FIGURE 1. System model.

priority into equilibrium to meet the backhaul transmission link construction of multiple BSs. The findings from our simulations reveal a clear enhancement in the performance of backhaul operations with our method, which has particularly notable effects in improving local minimum backhaul performance.

- 4) The UE strategies include two parts, UE distribution strategy and motion strategy, which aim to adapt to more algorithms and application scenes.

C. ORGANIZATION

This paper is organized as follows. It commences with an introduction to the system model and discussion of both the problem of UAV deployment and backhaul transmission link construction in Section II. Next, in Section III, we offer a resolution to the problem formulation. Then, in Section IV, based on simulation results, the superiority of our entire solution is demonstrated. Lastly, in Section V, we synthesize the key findings and summarize the contribution of each section.

II. SYSTEM MODEL

In this paper, we consider an uplink wireless communication system in an urban scenario where multiple users transmit data to a BS via an aerial UAV, consisting of N BSs, K UEs, and M UAVs, which can be deployed anywhere in the sky. UEs are ground-based communication devices uniformly distributed in a $2 \text{ km} \times 2 \text{ km}$ two-dimensional rectangular area, with BSs outside the area. We let $\mathbf{N} = \{1, 2, \dots, N\}$, $\mathbf{K} = \{1, 2, \dots, K\}$ and $\mathbf{M} = \{1, 2, \dots, M\}$ denote the set of terrestrial BSs, the set of terrestrial users, and the set of UAVs serving terrestrial UEs, respectively. It is assumed that all UAVs, BSs and UEs are equipped with omnidirectional antennas; for band allocation, it is assumed that BSs and UAVs operate in two mutually orthogonal bands and that all UAVs operate in mutually orthogonal bands with no interference between them. Each terrestrial UE can only be served by at least one UAV at a time; users have the same information transmission rate. In terms of the composition of the backhaul link, it is assumed that at a certain time, the UAV determines the best service location and can be connected to

a remote BS through a certain topology to form a multi-hop backhaul link, as shown in Figure 1, where C_i indicates that the UAV effectively transmits data traffic at the maximum transmission rate required for terrestrial users.

A. CHANNEL MODEL

Here we use UAV_i and UE_k to denote the i -th UAV and the k -th UE, respectively. For each UAV, the transmission channel between them in single link where they are directly connected to the UE is usually an A2G channel, and their connection may be blocked by obstacles, which can significantly degrade the transmission quality. Due to the complex terrain in which the UE is located, the channel between UAV and UE is typically represented by a LoS and NLoS probabilistic model [26], [27].

The probability of a LoS link between UAV_i and UE_k is:

$$P_{i,k}^{LoS} = \frac{1}{1 + a \exp(-b(\theta_{i,k} - a))}. \quad (1)$$

where a and b are the relevant environmental parameters and $\theta_{i,k}$ is the pitch angle between UAV_i and UE_k , which characterizes the relative altitude between them. $\theta_{i,k}$ can be obtained by calculating:

$$\theta_{i,k} = \frac{180}{\pi} \times \arctan\left(\frac{h_1 - h_0}{l_{i,k}}\right). \quad (2)$$

where h_1 represents the altitude of the UAV relative to ground level, h_0 represents the altitude of the UE relative to ground level, and $l_{i,k}$ represents the horizontal distance between UAV_i and UE_k . Since the UAV flies towards the BS at the same altitude as the UE, the relative altitude between UAV_i and UE_k is considered to zero.

The NLoS link probability between UAV_i and UE_k can then also be expressed as:

$$P_{i,k}^{NLoS} = 1 - P_{i,k}^{LoS}. \quad (3)$$

With both (1) and (3) defined, consequently, the A2G channel's link loss function can be represented in the following manner:

$$A_{i,k} = P_{i,k}^{LoS} \times PL_{i,k}^{LoS} + (1 - P_{i,k}^{LoS}) \times PL_{i,k}^{NLoS}. \quad (4)$$

where $PL_{i,k}^{LoS}$ and $PL_{i,k}^{NLoS}$ are the path loss of the LoS link and the NLoS link, respectively, which can be obtained from equations (5) and (6) below:

$$PL_{i,k}^{LoS} = 20 \lg r_{i,k} + 20 \lg f + 20 \lg \left(\frac{4\pi}{c}\right) + \mu_{LoS}. \quad (5)$$

$$PL_{i,k}^{NLoS} = 20 \lg r_{i,k} + 20 \lg f + 20 \lg \left(\frac{4\pi}{c}\right) + \mu_{NLoS}. \quad (6)$$

where μ_{LoS} and μ_{NLoS} are the mean additional path loss figures for LoS and NLoS channels caused by free space propagation loss, respectively. f denotes the carrier frequency of the channel between UAV and UE. $r_{i,k}$ denotes the

distance between UAV_i and UE_k , which can be obtained from equation (7) below:

$$r_{i,k} = \sqrt{h_0^2 + l_{i,k}^2}. \quad (7)$$

The absence of interference between UAVs and BSs is assumed due to the fact that both operate in two orthogonal frequency bands. UE_k can only be served properly if the total signal-to-noise ratio (SINR) between UAV_i and UE_k exceeds the threshold τ_r . This suggests that the UAV_i can guarantee both the transmission rate and the quality of service (QoS) for the UE_k . The SINR between the UAV and the UE can be calculated by the following equation:

$$\lambda_{i,k} = \frac{p_{i,k} G_{i,k}}{\sum_{m \neq i} p_{m,k} G_{m,k} + \sigma^2}. \quad (8)$$

where $p_{i,k}$ indicates the transmitted power between UAV_i and UE_k . $G_{i,k}$ denotes the channel gain of UAV_i and UE_k . σ^2 denotes the power of white gaussian noise.

In conclusion, there is an available and complete channel model that can be employed for analysis and calculation purposes. The proposed scheme's validity can be assessed by comparing it against this model. For ease of computation, we will utilize this channel model as the fundamental framework for analyzing the construction of backhaul transmission links.

B. CONNECTION MODEL

First, we assume that $\mathbf{M}_1 = \{UAV_i | i = 1, 2, \dots, n_u\}$ denotes all UAVs serving UEs and $\mathbf{K}_1 = \{UE_k | k = 1, 2, \dots, n_e\}$ denotes all terrestrial UEs. The SINR between UAV_i and UE_k can be obtained according to (8), which can be converted into units of dB for computational purposes and construct a two-dimensional SINR matrix of $n_u \times n_e$, which can be denoted as ζ^S , with element $\zeta_{i,k}^S$. We then construct the UE application tables and UE broadcast tables as two matrices of $n_u \times n_e$, which can be denoted as the ζ^{Bu} and ζ^{Be} , with elements $\zeta_{i,k}^{Bu}$ and $\zeta_{i,k}^{Be}$. Since there is a maximum number of UAVs and UEs, it is necessary to define two $n_u \times n_e$ matrices, which can be denoted as ζ_m^U and ζ_k^E respectively to represent the remaining unconnected slots for each UAV and UE.

The UE application table and the UE broadcast table will be updated to store a set of UAV_i with the largest SINR per UE and UE_k with the largest SINR per UAV, respectively. Here, we first update the UE application table by comparing UE_k with the SINR of each UAV to get the largest SINR of UAV_i and iterate through each UE. After this, it is equivalent to each UE sending a connection request to the UAV with the largest SINR between them, and since there are only two cases when a connection request is sent or not, we use 1 and 0 to indicate sent and unsent respectively for subsequent operations. At this point, the elements of the UE application table matrix ζ^{Bu} will represent the connection between each UAV and UE. Afterwards, we update the UE broadcast table by comparing UAV_i with the SINR between different UEs to get a set of UEs with the largest SINR

of UE_k , whose number is less than the maximum number of connections per UAV, and number the UEs obtained from each UAV according to their SINRs. At this point, the UE application table and the UE broadcast table have been updated and a simple sum of these two is all that is required to determine the connection status of the UAV and the UE. This is done until the UE application table and the UE broadcast table are matched with 0, which means that the UAV and UE connection status will remain unchanged, i.e. the connection balance will be maintained and no further connection operations will be performed.

C. PROBLEM FORMULATION

The main optimization objectives of our proposed model are to increase the UE service rate and maximize the effective backhaul rate in the region. We have divided the optimization problem into two problems for discussion as follows.

Problem 1 The optimization objective for increasing the service rate can be expressed as:

$$P_S : \max \sum_{i=1}^M \left(\frac{R_N}{M} \times m_i \right). \quad (9)$$

where m_i represents the number of UEs connected to each UAV. M and R_N are both constants, representing the total number of UAVs and the total demand rate for the region, respectively.

This section constructs the model with the following constraints:

$$S1 : \zeta_{i,k}^{Bu}, \zeta_{i,k}^{Be} \in \{0, 1\}. \quad (9a)$$

$$S2 : \zeta^U \leq n_u, \zeta^E \leq n_e. \quad (9b)$$

$$S3 : \zeta_{i,k}^S \geq 0. \quad (9c)$$

$$S4 : l_{i,k} \leq r_S, \forall i, k. \quad (9d)$$

$$S5 : \lambda_{i,k} \geq \tau_r, \forall i, k. \quad (9e)$$

$$S6 : n_u \leq M_{\max}. \quad (9f)$$

where (9a) indicates a logical constraint on whether the UE application table and the UE broadcast table are sent. (9b) indicates that the number of UAVs and UEs remaining unconnected should stay within the upper boundary for both. (9c) indicates that the SINR between UAV and UE must be greater than 0. (9d) indicates that the distance between UE and UAV which connected to UE should be less than the signal capture range of the UAV, otherwise the connection between them will not be maintained. (9e) indicates that the total SINR between the UAV and the UE needs to be greater than the threshold τ_r to maintain normal operation of the UE. (9f) indicates that the number of UAVs in the area does not exceed the set limit.

Problem 2 For the problem of maximizing the effective rate of backhaul transmission, we start with a directed graph of the backhaul network using $g_i(v_i, c_i)$ to represent the backhaul network that has been obtained, where $v_i = (x_i, y_i)$ represents the horizontal coordinates of the UAV, and $c_i = \{j \mid 1 \leq j \leq N\}$ represents the connected objects of the j

UAVs. From this, the backhaul path to UAV $_i$ can be obtained recursively, expressed as:

$$Q_i = [i, c_i, c_{c_i}, \dots, q_i^{-1}]. \quad (10)$$

where i represents the current UAV itself, as well as the location information v_i and the connection object information c_i , where q_i^{-1} represents a UAV that cannot be recursively continued in the backhaul path. Here the length of Q_i is set to L . The factor that restricts the optimization of backhaul transmission's effective rate is the maximization of UAV demand rate, which can be represented as:

$$UC : \max \sum_{i=1}^M RT_i^*. \quad (11)$$

where RT_i^* denotes the effective backhaul transmission rate of UAV $_i$. Through the equivalence of RT_i^* , (11) above can also be expressed as:

$$\max \sum_{i=1}^M \min \left(\min_{l=1,2,\dots,L-1} R_{i_l, i_{l+1}}, SC \right). \quad (12)$$

where i_l represents the l -th UAV in the backhaul transmission path of UAV, which can be denoted as Q_i . L represents the length of Q_i , and $R_{i_l, i_{l+1}}$ represents the maximum transmission rate between the l -th and $(l+1)$ -th UAVs. The constraint for the model constructed in this section is as follows:

$$S7 : c_i \neq \emptyset, 1 \leq i \leq M. \quad (12a)$$

$$S8 : q_i^{-1} = 0, 1 \leq i \leq M. \quad (12b)$$

$$S9 : i \notin Q_j, \forall j (j \neq i) \in Q_i, 1 \leq i \leq M. \quad (12c)$$

$$S10 : \sum_{i \in \{i \mid c_i = 0\}} RT_i^* + \sum_{j \in \{j \mid c_j \neq 0\}} RT_j^* \leq \sum_{i \in \{i \mid c_i = 0\}} R_{i,0}. \quad (12d)$$

where (12a) ensures that each UAV has a connection object. (12b) ensures that the information data transmitted by the link all reach the BS. (12c) ensures that no circular links are formed between different UAVs. (12d) ensures that only data from the A2G channel is transmitted on the A2A channel.

III. SOLUTION OF THE PROBLEM

A. BASIC IDEAS

To provide continuous and reliable service to the UEs in the hotspots, we first need to obtain the coordinates of the UEs in the hotspots. It is assumed here that the locations of the UEs can all be obtained from the prereleased UAVs. We then use the U-GWO algorithm to predeploy the UAVs in the area. After that, a U-AF model is established to analyze and predict the movement tendencies of the mobile UEs. In the process of UAV tracking UE motion trend, A2A and A2G backhaul links will be constructed. Since the congestion function in the traditional pure NE strategy considers non-zero values as quantity one, addressing the problem becomes more complex when using a centralized

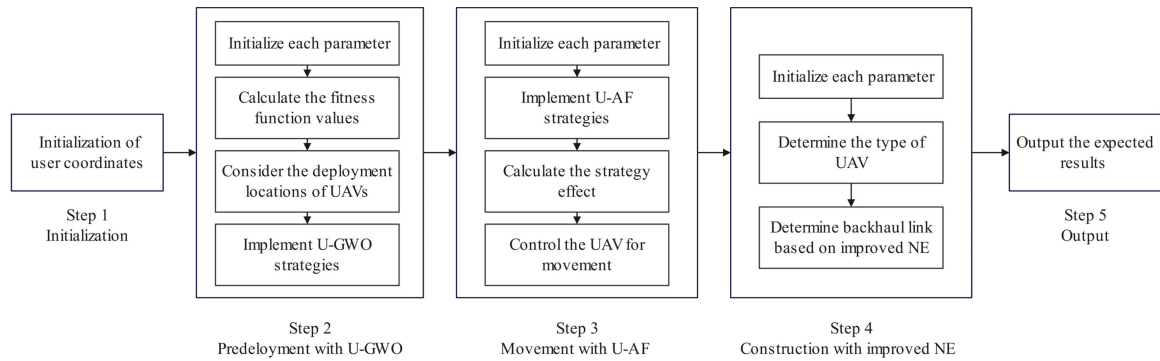


FIGURE 2. Flowchart of the overall solution realization.

approach. Therefore, to solve this problem, we will start with centralized and local optimization, preprocess the links first and then construct them with improved NE strategy. To provide a clearer understanding, the complete process of this scheme is shown in Figure 2 below.

B. UAV DEPLOYMENT AND MOBILE ALGORITHM

1) U-GWO ALGORITHM DESIGN

a: GWO ALGORITHM

GWO is a packet intelligence optimization algorithm proposed by Mirjalili et al. [28] in 2014, inspiring by the social intelligence of gray wolf (GW) packs in terms of leadership and hunting. For each pack of GWs, there is a common social hierarchy that determines the power and dominance of each pack member. The GWO algorithm divides the pack into four classes, namely wolves α , wolves β , wolves δ and wolves ω , with the strongest, i.e. the one with the most power, being wolves α , which leads the pack in hunting, migration and foraging. Weaker than the wolves α are the wolves β , which assist the wolves α in managing wolves δ and ω , and the wolves β will lead the pack when the wolves α is not in the pack, or dies of illness. The remaining wolves and wolves δ , ω are less powerful, with wolves ω being managed by wolves δ . This social intelligence is the main inspiration for the GWO algorithm. Another source of inspiration for the GWO algorithm is the way GWs hunt. When hunting their prey, GWs follow an effective set of methodological steps, which consists of chasing, encircling, harassing and attacking. This method of hunting allows them to hunt large prey.

b: SPECIFIC STEPS OF THE U-GWO ALGORITHM

For the optimization problem of deploying UAVs to assist terrestrial cellular networks, operators often need to invest in multiple UAVs. In order to address this issue, we propose the U-GWO algorithm, which offers a proficient approach to solve the UAV deployment problem and yield a range of optimal solutions. The notation used in this algorithm is summarized in Table 1.

Step 1: Initialize each parameter by importing the coordinates of UE.

TABLE 1. Symbols used in the U-GWO algorithm.

Symbols	Descriptions
$N = \{BS_j j = 1, 2, \dots, n_b\}$	Set of BSs
$M = \{UAV_i i = 1, 2, \dots, n_u\}$	Set of UAVs
$K = \{UE_k k = 1, 2, \dots, n_e\}$	Set of UEs
$G = \{GW_q q = 1, 2, \dots, n_g\}$	Set of GWs

Denote the maximum number of iterations, the number of GW populations and the maximum range of UAV services as I_{max} , n_g , r_{ser} and n_u . Initialize parameters I_{max} , n_g , r_{ser} and n_u . Construct a matrix ξ of $1 \times n_e$ to represent the contributions of all UEs, with each element of the matrix representing the contribution of the corresponding UE, and let the initial contribution of each UE be 1. Then construct a matrix ψ of $n_e \times n_g$, with element $\psi_{k,q}$ to represent the normalized distance relationship between each UE and the GW. If the distance between UE_k and GW_q is less than the maximum service distance of the UAV, r_{ser} , then $\psi_{k,q} = 1$, and vice versa $\psi_{k,q} = 0$.

Step 2: Calculate the fitness function values for all individuals in the GWs population.

We use the vector \mathbf{G} to represent the fitness of GWs, and for ease of representation, which can be calculated from the following equation (24):

$$\mathbf{G} = \xi \cdot \psi. \tag{13}$$

Step 3: Consider the deployment locations of UAVs with the highest fitness function values as wolves α , β and δ .

To obtain the best UAV deployment location, wolves need to be positionally guided, and since each wolf has a different ability to perceive the external environment, here wolves α , β and δ have a better perception of prey, which can be reflected in their higher fitness function values and more reliable to use as guides.

Step 4: GWs surrounding process.

During hunting, encircling prey can be represented by the following model:

$$D = |\mathbf{C} \cdot \mathbf{x}_{prey}(t_{it}) - \mathbf{x}(t_{it})|. \tag{14}$$

$$\mathbf{x}(t_i + 1) = \mathbf{x}_{prey}(t_{it}) - D \cdot \mathbf{A}. \tag{15}$$

where D represents the distance between prey and GW. $\mathbf{x}_{prey}(t_{it})$ and $\mathbf{x}(t_{it})$ represent the position vectors of prey and GW at the t_{it} -th iteration, respectively. \mathbf{C} and \mathbf{A} are the coefficient vectors, which can be calculated by the following equations, respectively:

$$\mathbf{C} = 2 \cdot \mathbf{r}_1. \quad (16)$$

$$\mathbf{A} = 2a \cdot \mathbf{r}_2 - a. \quad (17)$$

where $|\mathbf{r}_1|$ and $|\mathbf{r}_2|$ are the random numbers in the interval $[0, 1]$. In GWO algorithm, the convergence factor a has an initial value of 2 and decreases linearly to 0 according to $a = 2 - \left(\frac{t_{it}}{I_{\max}}\right)$ after entering an iteration. The relative distances of wolves ω to wolves α , β and δ can be calculated from the model constructed by (14) and (15) during GWs encirclement process. D_α , D_β and D_δ are the relative distances of wolves ω to wolves α , β and δ . Since wolves α , β and δ all travel different distances towards the target point and converge in different ways, the next positions of wolves ω are the average positions of wolves α , β and δ , respectively.

Step 5: GWs tracking process.

Since position updates of wolves ω during hunting are guided by wolves α , β and δ , the behavior of prey tracking can be described as:

$$\begin{cases} D_\alpha = |\mathbf{C}_1 \cdot \mathbf{x}_\alpha - \mathbf{x}| \\ D_\beta = |\mathbf{C}_2 \cdot \mathbf{x}_\beta - \mathbf{x}| \\ D_\delta = |\mathbf{C}_3 \cdot \mathbf{x}_\delta - \mathbf{x}| \end{cases} \quad (18)$$

where D_α , D_β and D_δ represent the distances from wolves ω to wolves α , β and δ , respectively. \mathbf{C}_1 , \mathbf{C}_2 and \mathbf{C}_3 are vectors of coefficients of random numbers generated in $[0, 1]$. \mathbf{x}_α , \mathbf{x}_β , \mathbf{x}_δ and \mathbf{x} are vectors of the current positions of wolves α , β , δ and ω , respectively. In each iteration, the positions of the wolves ω are updated and improved based on the positions of wolves α , wolves β and wolves δ :

$$\begin{cases} \mathbf{x}_1 = \mathbf{x}_\alpha(t_{it}) - D_\alpha \mathbf{A}_1 \\ \mathbf{x}_2 = \mathbf{x}_\beta(t_{it}) - D_\beta \mathbf{A}_2 \\ \mathbf{x}_3 = \mathbf{x}_\delta(t_{it}) - D_\delta \mathbf{A}_3 \end{cases} \quad (19)$$

$$\mathbf{x}(t_{it} + 1) = \frac{\mathbf{x}_1 + \mathbf{x}_2 + \mathbf{x}_3}{3}. \quad (20)$$

where (19) specifies the direction and step size of the movement of wolves ω to wolves α , β and δ , and (20) indicates the final position of wolves ω .

Step 6: Output the optimal solution position.

After updating all positions of wolves ω , we recompute the fitness function for all wolves ω and can obtain the optimal three solutions in the t_{it} -th iteration, as expressed in the following equation:

$$\begin{aligned} j_{i,1} &= \arg \max_{j \in J} (\mathbf{G}) \\ j_{i,2} &= \arg \max_{j \in \{J \cap j_{i,1}\}} (\mathbf{G}) \\ j_{i,3} &= \arg \max_{j \in \{J \cap j_{i,1} \cap j_{i,2}\}} (\mathbf{G}) \end{aligned} \quad (21)$$

Algorithm 1 The U-GWO Algorithm.

```

1: Initialize  $t_{it} = 0$ .
2: Initialize the GW population  $GW_q$ .
3: Initialize  $a$ ,  $\mathbf{A}$  and  $\mathbf{C}$ .
4: for  $j = 1 : n_u$  do
5:   Calculate the fitness of each search agent.
6:    $X_\alpha =$  The best search agent.
7:    $X_\beta =$  The second-best search agent.
8:    $X_\delta =$  The third-best search agent.
9:   for  $t_{it} = 1 : I_{\max}$  do
10:    for
11:      each search agent do
12:        Update the position of the current search agent
13:        according to (15).
14:      end for
15:      Update  $a$ ,  $\mathbf{A}$  and  $\mathbf{C}$ .
16:      Calculate the fitness of all search agents.
17:      Update  $X_\alpha$ ,  $X_\beta$  and  $X_\delta$ .
18:      Let  $t_{it}++$ .
19:    end for
20:  end for
Output:  $X_u$ .

```

where $j_{i,1}$, $j_{i,2}$ and $j_{i,3}$ denote the positions of the wolves ω for the t_{it} -th iteration, respectively. The set of all positions of wolves ω is defined as $J = \{1, 2, \dots, n_g\}$. Then, until the maximum number of iterations is reached, we replace the previous positions of wolves α , β and δ when a better solution appears in the iteration. When the maximum number of iterations is reached at I_{\max} , the optimal solution is the location of the wolves α , and the set of corresponding UAV locations is finally output as X_u .

2) DESIGN OF U-AF MODEL

The anti-flocking model [29] is derived from the fact that creatures in nature are used to living alone, such as brown bears, leopards, lynxes, spiders and etc. Different from the clustering behavior of ants, bees and wolves, which prefer to live and hunt apart from each other and own their own living space. At the same time, if an outsider enters their living space, they will react to defend their living space. To more effectively track and predict moving targets in mobile surveillance systems, Miao et al. [30] described solitary organism habits as anti-flocking and summarized it in two properties:

1) Profitability. Solitary organisms will maintain their hunting habits for the greatest possible gain without outside interference.

2) Avoidance. Solitary organisms spatially avoid as many adverse effects on themselves as possible, such as foreign organisms or other obstacles.

As UAVs operating in the air need to track the location of UEs on the ground to maximize service coverage,

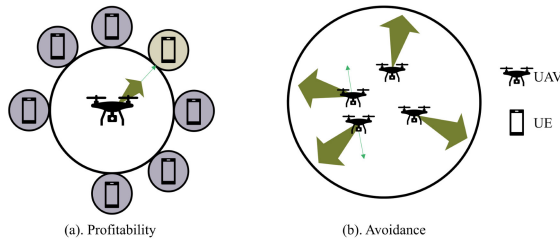


FIGURE 3. Two rules of anti-flocking algorithm: a) Profitability, b) Avoidance.

there may be interference or collision risks between UAVs that are too close to each other, we design a user-aware anti-flocking model for UAV deployment as shown in Figure 3 below. Clearly, there are similarities between the behavior of normally operating UAVs and the habitat characteristics of solitary organisms, so it is reasonable to apply the anti-flocking model to the multi-UAV movement and deployment model. The following section will describe the composition and construction of the U-AF model.

a: UE HUNTING STRATEGY

Firstly, each UAV has its own range of prey, R_h , and the UAV can sniff out all UEs which exist in this range and record the number of these UEs. The total count of UEs and the vectorial sum of the individual vectors directed from UAV to UEs can be denoted as m_{py1} and \mathbf{P}_1 , respectively. Secondly, as UEs move, the UAV updates the total count of UEs in its own hunting range R_h and the vectorial sum of the individual vectors directed from UAV to UEs, can be denoted as m_{py2} and \mathbf{P}_2 , respectively.

We assume that the hunting effect parameter of UAV is h_1 , then the effect of hunting strategy of UAV subject to the direction of the motion trend of UE can be expressed as:

$$\mathbf{H} = h_1 \times \frac{\mathbf{P}}{m_{py1}} \tag{22}$$

where \mathbf{P} is the sum of the vectors \mathbf{P}_1 and \mathbf{P}_2 .

b: UAV HIDING STRATEGY

Since each UAV will respond to other UAVs that enter its hunting range at R_h and are not larger than its safe distance, the stress here is expressed as a repulsion between UAVs to avoid possible negative effects of being too close. We assume that each UAV can sniff out other UAVs that come into the range of R_h . The safe distance between two UAVs is assumed to be R_{ser} and the avoidance parameter is h_3 . The direction vector between UAVs with a distance less than R_h , can be set to \mathbf{D} . Then the amount of hiding strategy of the UAV to avoid the impact from other UAVs can be expressed as:

$$\mathbf{E} = \begin{cases} h_3 \left(1 - \frac{R_{ser}}{|\mathbf{D}|} \right) \times \frac{\mathbf{D}}{|\mathbf{D}|}, & (|\mathbf{D}| < R_{ser}) \\ 0, & (R_{ser} \leq |\mathbf{D}|) \end{cases} \tag{23}$$

c: UAV SELFISH STRATEGY

For each UAV, if no other UAV enters its hunting range R_h when it is tracking UE, i.e. executing the UE hunting strategy, it will have no effect on its original strategy and the UAV will maintain its previous movement to maximize the coverage of UE. If a situation arises while executing UE hunting strategy that causes the UAV to evade, it will execute UAV hiding strategy until the conditions for the execution of UAV hiding strategy are no longer satisfied and will again commit to the execution of the UE hunting strategy. Thus, the UAV selfish strategy serves to make the UAV hiding strategy and the UE hunting strategy executable in succession. Meanwhile there is no needs to constrain the execution of the two main UAV strategies in terms of time and order of execution.

d: UAV STRATEGY EFFECT PROPAGATION SPEED

Given that the UAV has a limited speed, we associate the received strategies with the speed of the UAV through a mapping. Here, let's suppose that the UAV has a maximum speed of V_{max} , and receives the sum of strategies is \mathbf{S} at any given moment. The speed at which the strategy effect propagates can be calculated as:

$$\mathbf{v} = \frac{2}{\pi} \times V_{max} \times \arctan(|\mathbf{S}|) \times \frac{\mathbf{S}}{|\mathbf{S}|} \tag{24}$$

C. BACKHAUL TRANSMISSION SCHEME

1) LINK PREPROCESSING

Considering that the utility function is not optimal for the construction of backhaul links, e.g. UAV_i and BS_j get closer together until $R_{i,j}$ is larger than P_{S_i} , there may still be $c_i = 1$. Obviously, this will reduce the value of P_{S_i} when it comes to:

$$\sum_{i=1}^M RT_i^* = \sum_{j \in \{j|c_j \neq 0\}} RT_j^* + \sum_{i \in \{i|c_i = 0\}} RT_i^* \tag{25}$$

Therefore, this paper categorizes UAVs into two groups, resident UAVs and non-resident UAVs, which can be expressed as:

$$U^S = \{i | R_{i,j} \leq P_{S_i}, 1 \leq i \leq M\} \tag{26}$$

$$U^{IS} = M - U^S \tag{27}$$

where U^S and U^{IS} denote resident UAV and non-resident UAV, respectively.

2) BACKHAUL TRANSMISSION LINK COMPOSITION ALGORITHM BASED ON AN IMPROVED NE STRATEGY

In 1944, von Neumann and Morgenstern published their seminal work, "Game Theory and Economic Behaviour," which pioneered the interdisciplinary field of game theory. Since then, game theory as a study of strategic decision-making has been widely used not only in various disciplines but also in our daily lives. As a key concept for noncooperative games,

Algorithm 2 UE Tracking Based on the U-AF Algorithm.

```

1: Initialize  $T_{\max}, R_h, V_{\max}$  and  $v_{ue}$ .
2: Initialize  $a, b, n_u$  and  $n_e$ .
3: Initialize  $t = 0, n = 0$ .
4: for  $n = 1 : n_u$  do
5:   UAV hunts all UEs within the range of  $R_h$ .
6:   UAV records  $m_{py1}, \mathbf{P}_1$  and the number of all captured UEs.
7: end for
8: for  $t = 1 : T_{\max}$  do
9:   for  $n = 1 : n_e$  do
10:    All UEs move at  $v_{ue}$ .
11:   end for
12:   for each UAV do
13:    UAV records  $m_{py2}, \mathbf{P}_2$  and calculates  $\mathbf{P}$ .
14:    UAV calculates the effect of hunting strategy according to (22).
15:    UAV calculates the effect of hiding strategy according to (23).
16:   end for
17:   for each UAV do
18:    UAV hunts all UEs within the range of  $R_h$ .
19:    UAV records  $m_{py1}, \mathbf{P}_1$  and the number of all captured UEs.
20:   end for
21:   Record and update the service rate in this iteration.
22: end for

```

NE, which denotes an action profile in which no player can gain more payoff by changing its own action provided that the rest of the players keep their actions, has been widely adopted to depict the outcome of strategic interactions for noncooperative games ever since the seminal result. Game theory describes NE as a process of game formation in which the NE represents the execution of all individuals in the execution of their strategies, meaning that the whole system reaches NE when all individuals believe that there will be no change that is more appropriate for them while the environment they are in remains the same, and individuals will be satisfied with their current strategies [31]. We will find the NE point of the backhaul transmission efficiency obtained by the UAV, that is, updating the combination of backhaul links constructed by the non-resident UAV until we find the NE point of the objective function. Therefore, it is necessary to find a useful function to determine whether the system under study has reached a NE point. This utility function [32] is denoted as:

$$u_i(g) = \frac{\sqrt{\min_{l=1,2,\dots,L-1} R_{i,l+1}}}{\Gamma_{i,Q_i}(g)^{0.3}}. \quad (28)$$

where g is a simplified representation of $g(v, c)$. $\Gamma_{i,Q_i}(g)$ represents the level of congestion on the UAV_{*i*} backhaul

path Q_i , which can be expressed as:

$$\Gamma_{i,Q_i}(g) = \sum_{l=1,2,\dots,L-1} \left(\frac{\rho_{il} + 2(R_{i,l+1} - \rho_{il})}{2R_{i,l+1}^2 - 2\rho_{il}R_{i,l+1}} \right). \quad (29)$$

where ρ_{il} indicates the rate of data received by the l -th UAV in the backhaul transmission path Q_i . Note here that if $R_{i,l+1}$ is less than ρ_{il} , $\Gamma_{i,Q_i}(g)$ under any $(i, l+1)$ belonging to Q_i will be assigned with -1 to signify that the result is not valid.

The connection information of UAV_{*i*}, which can be denoted as c_i , can be considered as the current connection strategy for UAV_{*i*}, so that the overall strategy with local NE for UAV_{*i*} can be expressed as:

$$c^{NE} = (c_i^{NE}, c_{-i}^{NE}) = (c_1^{NE}, c_2^{NE}, \dots, c_M^{NE}). \quad (30)$$

The equation here represents a state in which UAV_{*i*} does not change its current connection strategy c_i while the connection strategies of other UAVs, c_{-i} stay consistent, and concurrently, the connection strategies of other UAVs, c_{-i} cannot change considering the current situation.

Subsequently, the connection strategy can be integrated with the NE algorithm through the utility function. The connection strategy that maximizes utility function of each UAV can be identified as the target strategy to determine the NE point for each UAV. Given that only UAVs that are not resident in a specific location are considered in the NE strategy process, this can be mathematically expressed by the following equation:

$$c_{i \in U^{IS}}^{NE} = \begin{cases} \arg \max u_i(g) & \text{if } \exists u_i(g) \geq 0 \\ c_i & \text{else} \end{cases} \quad (31)$$

In the process of determining the NE point for each UAV, the UAVs will establish connections with other UAVs sequentially in a circular manner through contact composition until (31) above is satisfied. When a particular UAV_{*i*} has obtained its NE point, there is $(c_i, c_{-i}) \Rightarrow (c_i^{NE}, c_{-i}^{NE})$, where c_i^{NE} satisfies (31). Consequently, regardless of the situation, as long as the other UAVs maintain their existing connection strategies c_{-i} , c_i^{NE} will not change. In turn, when all UAVs have satisfied the NE, this means that the last UAV has also found its NE, at which point all UAVs will remain in NE, i.e. $c = (c_i, c_{-i}^{NE}) \Rightarrow c^{NE} = (c_i^{NE}, c_{-i}^{NE})$, here c_i^{NE} for all $i \in U^{IS}$, satisfying (31), and the whole system will reach a steady state.

Due to the requirement of maintaining the environment invariant feature for NE strategies of each UAVs, only one UAV can be involved in the NE process at a time, i.e. only one c_i finds the corresponding c_i^{NE} at a time. We use $c^t = (c_i^t, c_{-i}^t) = (c_1^t, c_2^t, \dots, c_M^t)$ to denote the global connectivity strategy at time t . Then for any time $t + 1$, there is only one UAV that is non-resident and takes part in the NE process $c^t = (c_{i \in U^{IS}}^t, c_{-i}^t) \Rightarrow c^{t+1} = (c_{i \in U^{IS}}^{NE}, c_{-i}^{t+1})$, here $c_{-i}^{t+1} = c_{-i}^t$, and $c_{j \in U^{IS}}^{NE} \subseteq c_{-i}^t$.

Based on the arguments for global strategies under time-varying games in [33], we can obtain that under time-varying games, there exists a time t^* such that the system

reaches a NE, when the global strategy can be expressed as:

$$c^{t*} = (c_1^{t*}, c_2^{t*}, \dots, c_M^{t*}) = c^{NE} = (c_i^{NE}, c_{-i}^{NE}). \quad (32)$$

In the NE process, from time t to $t + 1$, there is $c^t = (c_{i \in U^{IS}}^t, c_{-i}^t) \Rightarrow c^{t+1} = (c_{i \in U^{IS}}^{NE}, c_{-i}^{t+1})$ and UAV $_i$ gets its NE point. However, when goes from time $t + 1$ to $t + 2$, there is $c^{t+1} = (c_{j \in U^{IS}}^{t+1}, c_{-j}^{t+1}) \Rightarrow c^{t+2} = (c_{j \in U^{IS}}^{NE}, c_{-j}^{t+2})$, and the environment changes due to $c_j^t \in c_{-i}^t$, i.e. $c_j^{NE} \in c_{-i}^{t+1}$ and there may be $c_i^{t+1} \neq c_i^{NE}$ at this point. This leads to an unsuccessful NE, requiring the UAV to undergo the NE process once more. To address this issue, we define the sum of one NE process involving each non-resident UAV as one iteration, and denote the backhaul transmission link after the iteration as $g_{it}(v, c)$.

Since only one UAV participates in the NE process at each time t is added, we will use the probability density approach within the hybrid NE strategy to ensure the systematic engagement of all UAVs in the process [31]. Moreover, considering that each non-resident UAV is limited to participating in the NE process only once during each period, we can establish the following definition. We denote $\Phi(t)$ as all sequences of UAVs waiting to participate in the NE process at time t in each iteration. Then each UAV $_i$ participation is followed by $\Phi(t) = \Phi(t - 1) - i$ with initialization of $\Phi(0) = U^{IS}$. Here $p(c_i^t)$ denotes the probability that UAV $_i$ participates in the NE process as time t increases. Since $p(c_i^t)$ is introduced here, it is also obvious that a corresponding restriction needs to be introduced here:

$$\sum_{i=1}^M p(c_i^t) = 1. \quad (33)$$

Furthermore, A2A links are accessible only when the maximum demand rate of UAVs is completely fulfilled in the NE process. Even if the maximum demand rate of most UAVs can be met by an A2A link, it still cannot be accessed and will be rejected if the overall maximum demand rate is not satisfied. Here we denote such UAVs that cannot be accessed as U^{RJ} , and those that can access the link as U^{NRJ} . In the NE process, only U^{NRJ} can contribute positively to improving the optimization of backhaul transmission rate. Here we can obtain a form of maximizing the transmission rate:

$$UC : \max_{g(v,c)} \sum_{i \in U^{NRJ}} SC. \quad (34)$$

Here, since the maximum service rate SC will be determined under UAV deployment determination and U^{NRJ} is obtained after $g_{it}(v, c)$ is determined, this problem is equivalent to maximizing U^{NRJ} , specifically, as long as the non-resident UAVs participating in the NE process meet the following criteria as time t increases during each iteration:

$$\begin{cases} p(c_{i^*}^t) = 1, i^* = \arg \max \|(x_i, y_i) - (x_j, y_j)\| \\ p(c_{-i^*}^t) = 0 \end{cases} \quad (35)$$

Algorithm 3 Backhaul Transmission Link Composition Algorithm Based on Improved NE Strategy.

- 1: Initialize $g_{it}(v, c)$.
- 2: Initialize $t_{it} = 0, c_i = 0, i \in M$.
- 3: Categorize UAVs into U^S and U^{IS} according to (26)(27).
- 4: Initialize $\Phi(t = 0) = U^{IS}$.
- 5: **while** $\Phi(t) \neq \emptyset$ **do**
- 6: Get the value of i^* that is involved in NE process as derived from (35).
- 7: Calculate the strategy associated with i^* once it achieves NE according to (31).
- 8: Update strategy $c^t = (c_{i^*}^t, c_{-i^*}^t) \Rightarrow c^{t+1} = (c_{i^*}^{NE}, c_{-i^*}^{t+1})$.
- 9: Let $t++$.
- 10: Obtain $\Phi(t) = \Phi(t - 1) - i^*$.
- 11: **end while**
- 12: Let $t_{it}++$.
- 13: Store the backhaul transmission link $g_{it}(v, c)$ formed by this iteration.
- 14: Until $\exists t_{it}^* < t_{it}, g_{it}(v, c) = g_{it^*}(v, c)$.

Output: $g_{it}(v, c)$ and U^{RJ} .

where (x_i, y_i) and (x_j, y_j) denote the two-dimensional coordinates of UAV $_i$ and BS $_j$, and $i \in \Phi(t)$. This strategy suggests that the NE process will prioritize the participation of the UAV located farthest away from the BS.

With the probabilistic allocation strategy shown in (35), subsequently, a sequence of non-resident UAVs is determined through the NE process in each iteration. Based on this sequence, the connection strategy for each of the participating UAVs in the NE process is updated by (31) until $\Phi(t) \neq \emptyset$. Afterwards, the iteration cycle continues until the newly established backhaul transmission link matches the same as the previously established backhaul transmission link.

IV. PERFORMANCE SIMULATIONS

In this section, we evaluate the performance of the UAV access deployment algorithm by first comparing the impact of using different swarm intelligence optimization algorithms on the UAV predeployment results, i.e. the differentiation of the UAV user service rate. In addition, we also compare the maximum UE service rate under different algorithms, considering the different switching speeds and number of UEs in the hotspots where the movement occurs. To evaluate the efficiency of UAV backhaul transmission link information transmission, we compare the influence of various scenarios on the backhaul performance of the system and offer a comprehensive analysis. Here, we consider UEs are distributed in an area of 2 km \times 2 km, and moving at v_{ue} , the average effective backhaul rate of the system is R_{av} , the minimum effective backhaul transmission rate is R_{min} and the signal transmission power of the UAV is P_{trans} . Here R_{av} represents the improvement in the overall performance

TABLE 2. Simulation parameters.

Parameters	Value
a	9.6
b	0.28
f	2 GHz
μ_{LoS}	1 dB
μ_{NLoS}	20 dB
σ^2	-90 dBm
τ_r	-5 dB
R_h	500 m
R_{ser}	230 m
n_u	40
n_e	40
I_{max}	400
h_1	2
h_3	1000
V_{max}	10 m/s
h_{uav}	100 m
h_{bs}	0 m
v_{ue}	1 m/s

of the system and R_{min} represents the improvement in the balanced performance of the system. The algorithms are evaluated using Windows 11 and MATLAB. All simulations are conducted on a laptop equipped with an AMD Ryzen 5 6600H CPU with Radeon Graphics, running at a clock speed of 3.3 GHz. The simulation parameters are shown in Table 2.

A. EFFECTIVENESS OF UAV DEPLOYMENT BASED ON U-GWO ALGORITHM AND COMPARISON WITH OTHER ALGORITHMS

Considering that the primary evaluation metric for assessing the performance of the UAV access deployment algorithm is the service rate of UE in the region, we will calculate the average value based on multiple simulations. This approach ensures the accuracy of the results obtained. As shown in Figure 4 below, we have the purely dispersed distribution, mixed centralized-decentralized distribution and purely centralized distribution of UEs, with their result maps after predeployment by the U-GWO algorithm, respectively. Since we study UAV deployment in hotspots, the results of the subsequent experiments are all based on the mixed centralized-decentralized distribution of UEs. First, we investigate the deployment performance of U-GWO. In the experiments conducted for this paper, we create three hotspot areas within the target region. Each hotspot area has a different radius and contains a varying number of UEs. The remaining vacant area is populated with dispersed individuals. We set the total number of UEs and the total number of deployable UAVs in the region to 400 and 10, respectively. The randomly generated UE distribution map of the hotspot area and the resulting UAV deployment map implemented according to the U-GWO algorithm are shown in Figure 4. Figure 4 (a) shows the randomly generated UE distribution map, wherein the blue dots indicate UEs, while Figure 4 (b) shows the result map after predeployment by the U-GWO algorithm, wherein the UEs in Figure 4 (a)

are indicated by blue dots and the red circles indicate the predeployed UAVs.

As shown in Figure 4, after deploying the target area with U-GWO algorithm, UAVs are deployed reasonably evenly in hotspots, where more UAVs will be deployed for hotspots in clusters with a larger number of UEs, fewer UAVs will be deployed for hotspots in clusters with a smaller number of UEs, and for areas that are more dispersed or contain no UEs. In order to further illustrate the effectiveness of the U-GWO algorithm, we conduct a comparative analysis with other cluster intelligence optimization algorithms. The metric used for comparison in this study is the UE service rate.

Here we begin with a brief description of the algorithms that will be compared. The algorithms compared include Sparrow Search Algorithm (SSA), Whale Optimization Algorithm (WOA), Slime Mould Algorithm (SMA), and Chimpanzee Optimization Algorithm (ChOA). Here, we do an analogous treatment of these algorithms to the U-GWO algorithm so that they are applied to UAV deployments, they can be noted as U-SSA, U-WOA, U-SMA and U-ChOA, respectively, as shown in Figure 5.

As can be seen from Figure 5 (a), when the number of UEs in the hotspot is 400, the U-GWO algorithm is more stable and superior when the number of UAVs varies between 5 and 10 compared to the algorithm used for comparison. When the number of UAVs varies, the U-GWO algorithm can guarantee maximum UE service rate. As can be seen from Figure 5 (a), the overall service rate of the algorithms tested here is close when the number of UAVs is set to 7 and below, but when the number is increased to 8 and above, the difference between the algorithms becomes apparent. U-ChOA is more effective than U-SSA when the number of UAVs is 8, but less effective than U-SSA when the number of UAVs reaches 9. The overall observation is that the results obtained by the U-GWO algorithm tend to grow linearly when the number of UAVs increases from 5 to 10, and when the the total number of UAVs reaches 9, the maximum service rate obtained by other algorithms is saturated, while U-GWO still shows a growing trend, and in the subsequent experiments, we increase the number of UAVs to 16 and above before the results obtained by UAVs reach saturation. This is a good indication of the effectiveness of the U-GWO algorithm in deployment.

From Figure 5 (b), it can be seen that when the number of UEs in the hotspot area is 400 and the number of iterations of the algorithm varies between 50 and 400, the service rate obtained using the U-GWO algorithm is 80 % of the largest one and 71.2 % when the number of iterations is 50. The overall service rate shows an increasing trend as the number of iterations increases. The other algorithms show results that are less effective than the proposed U-GWO algorithm. U-SMA is relatively stable but has a low service rate of 65 %. U-SSA, U-WOA and U-ChOA have a maximum service rate of 75.2 % (U-WOA) and a minimum value of 67.4 % (U-ChOA), but are still less effective and less stable than the U-GWO algorithm. Overall, the U-GWO algorithm we have chosen is more effective and stable than the other algorithms.

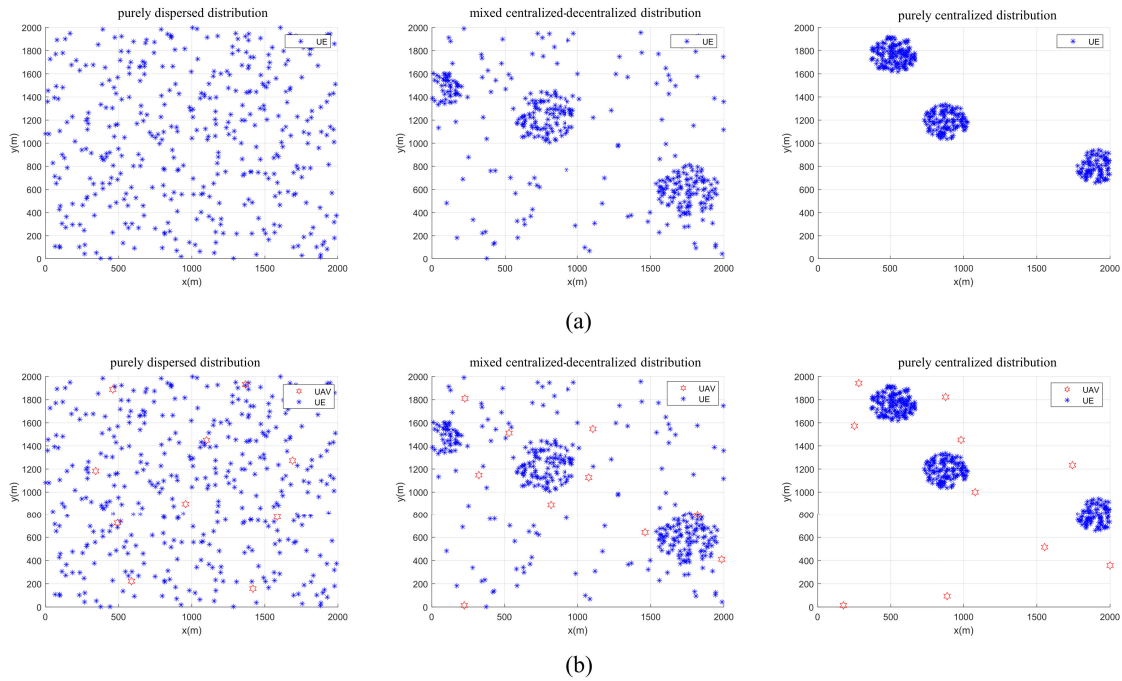


FIGURE 4. The UE distribution map. (a) before deployment of the U-GWO algorithm. (b) after deployment of the U-GWO algorithm.

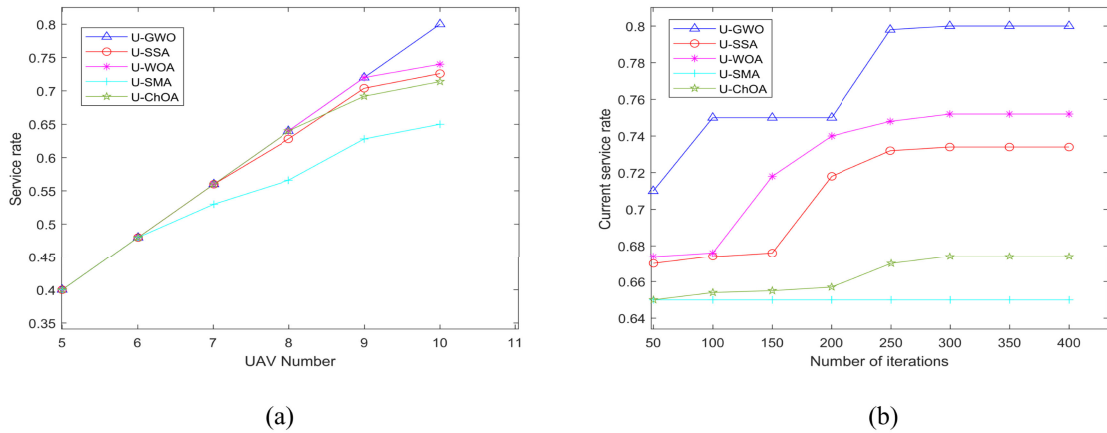


FIGURE 5. Service rate of UEs with different deployment algorithms.

As can be seen from Figure 6, when the number of UAVs in the hotspot area is fixed at 10, the U-GWO algorithm is more stable and superior when the number of UEs varies in the interval from 100 to 600 compared to the algorithm used for comparison. Considering that the test environment is a 2 km × 2 km rectangle, the number of UEs can directly reflect the UE density in the area, so here we use the change in the number of UEs to characterize the change in UE density. The U-GWO algorithm can guarantee the maximum service rate of UE to be high when the number of UEs varies. From Figure 6, it can be seen that the overall service rates of the algorithms tested here are close when the number of UEs

is set to 200 and below, but when the number exceeds 200, the gap between the algorithms becomes evident. When the number of UEs is less than 200, the difference in service rates obtained by the algorithms is not significant, because the number of UAVs is sufficient to cover the current number of UEs with a sufficient distribution of locations in the region to clearly demonstrate the superiority of the predeployment algorithms. However, as the number of UEs increases, the performance of each algorithm tends to diminish. The service rate obtained by U-GWO is greater than the results of the other algorithms, and the minimum value is still available at 65.3 %. When the number of UEs is at 600, the maximum

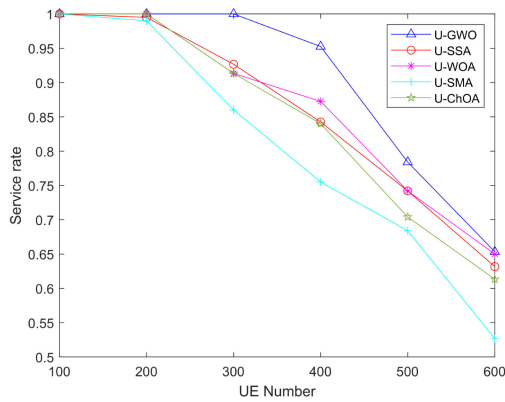


FIGURE 6. Service rate of UE with different UE number.

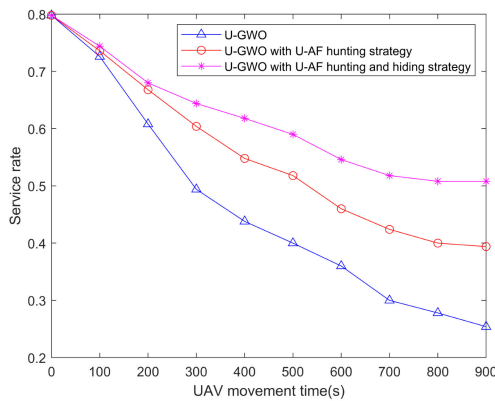


FIGURE 7. Service rate of UEs with different UAV tracking strategies ($v_{ue} = 1 \text{ m/s}$).

value of the service rate obtained with the other algorithms is 63.1 % and the minimum value is 52.6 %. This shows that U-GWO is more adaptable and effective than the other algorithms when the number of UE changes.

B. EFFECTIVENESS OF U-AF STRATEGY IMPLEMENTATION IN UE HOTSPOT AREAS

In order to examine the effectiveness of the U-AF strategy on UEs in the hotspot area, we create a larger hotspot by combining three smaller hotspots with varying numbers of UEs. As the hotspot moves, the average service rate of UEs in the target area changes in response to the varying number of UEs. Figure 7 below shows the results of predeployment with the U-GWO algorithm, with different combinations of U-AF strategies during UE movement.

Figure 7 shows the effect of using different combinations of strategies on the UE service rate for a certain number of UEs moving within the target area, moving with 1000 s in total. The final results show that at the early stage of UE movement, i.e. when the UE movement time is less than 100 s, the service rate results obtained for the three strategies compared are similar. This is because the UE speed is limited and the UE moves a smaller distance in a shorter period, the position of the UE after movement obtained at this time is close to the

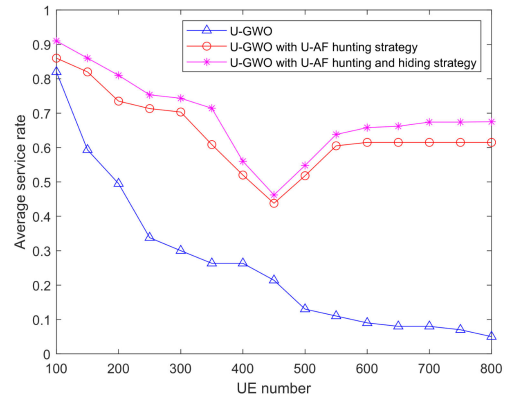


FIGURE 8. Average service rate of UEs with different number of UEs ($v_{ue} = 1 \text{ m/s}$).

position where the UE does not move, making the UAV less effective in tracking the UE. When the UE movement time reaches 200 s, there is a greater gap between the solution without U-AF strategy and the solution with U-AF strategy, and the minimum gap is 6 %. When the UE movement time reaches 300 s and above, the maximum service rate obtained by the solution with both U-AF hunting and hiding strategies is higher than that of the solution without U-AF and the solution with only U-AF hunting strategies, the maximum service rate obtained by the scheme with both U-AF hunting and hiding strategies is 25.4 % and 11.4 % higher, respectively. This shows that U-AF is effective in achieving the maximum service rate in the case of UE movement, and further demonstrates the need to use both hunting and hiding strategies in U-AF.

The graphical representation in Figure 8 shows how different combinations of strategies affect the average service rate of UEs as they move in the target area, considering variations in the number of UEs. The final results show that the average UE service rate is improved by 37.7 % and 43.2 % with only the hunting strategy in U-AF and with both hunting and hiding strategies in U-AF, respectively, comparing to U-GWO predeployment without U-AF. When the number of UEs is around 100, the results are similar with U-AF or not at this time because when the number of UEs is small, there will still be more UEs in the predeployed UAV range after the UAV predeployment has been executed, considering the UE movement speed limit. However, when the number of UEs exceeds 100, it becomes apparent that the average service rate of UEs without U-AF strategy will decrease significantly, while the results with U-AF vary more steadily. When the number of UEs reaches 450, a clear inflection point in the curve with the U-AF strategy is noticed, which indicates that UAV can use the U-AF strategy to capture the movement trend of UEs if the number of UEs increases significantly, or when there is a large influx of UEs, so that the hotspot movement can be tracked effectively. As a result,

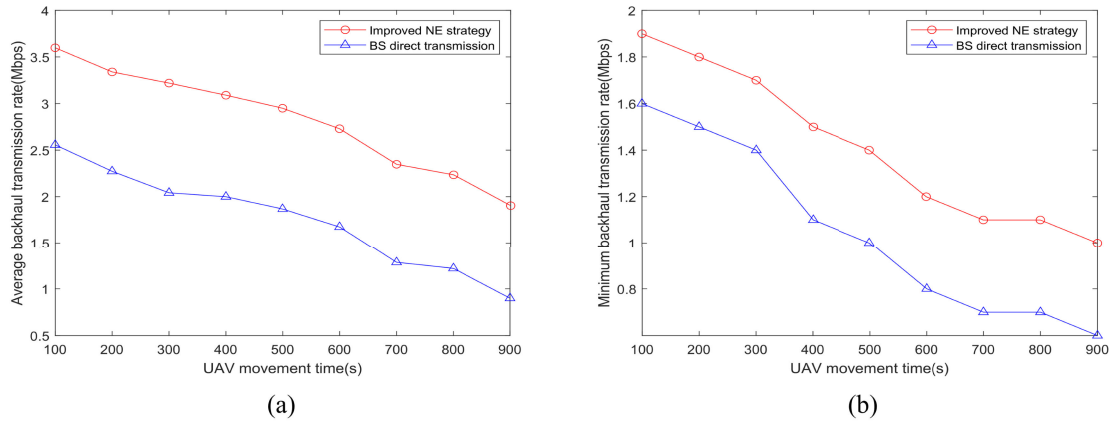


FIGURE 9. The average and minimum backhaul transmission rate of dynamic backhaul links under different schemes.

the connection pressure on the terrestrial BSs can be relieved to a large extent.

C. EFFECTIVENESS OF CONSTRUCTING THE BACKHAUL TRANSMISSION NETWORK WITH IMPROVED NE STRATEGY

Considering that during the UE movement, the UAV will adopt U-AF strategy to track the UE position to obtain the maximum service rate, but at this time, due to the movement of UAV, the distance between it and our preset BS will change, making the demand rate of each UAV be different, thus leading to the change of the effective transmission rate of the backhaul transmission link constituted by the UAV at the current moment. To validate the reliability and effectiveness of our proposed algorithm for dynamic backhaul transmission link establishment, we positioned two BSs at fixed coordinates (1000, 1800) and (1200, 1200) within the designated area. The UEs will make movements away from the BSs and, therefore, the UAVs will also move away from the BSs, at which point we compare here the average effective backhaul transmission rate and the minimum effective backhaul transmission rate using different backhaul transmission link construction methods. The results of this comparison are shown in Figure 9.

As shown by the results in Figure 9, both the average effective backhaul transmission rate R_{av} and the minimum effective backhaul transmission rate R_{min} decrease as the UAV gradually moves away from the BS. As shown in Figure 9 (a), during the movement of the UAV, the average effective backhaul transmission rate R_{av} shows a decreasing trend for both the scheme with a directly connected BS and the scheme with an improved NE strategy, but the overall effect of the scheme with an improved NE strategy is better than that of the scheme with a directly connected BS, where the minimum value of the scheme with an improved NE strategy is 1.8 Mbps, which is 125 % higher than that of the scheme with a directly connected BS, which is 0.8 Mbps. In Figure 9 (b), the minimum effective backhaul

transmission rate R_{min} for both compared schemes also shows a decreasing trend, but the decrease is higher for the direct BS scheme than the improved NE scheme, and the minimum value for the former is 0.6 Mbps and the latter is 1 Mbps, which is 67 % higher than the former, indicating that the improved NE scheme is more stable and achieves a higher effective backhaul transmission rate. The effective backhaul transmission rate is greater and the results are better, which also proves the superiority of our proposed scheme.

After comparing the direct BS connection scheme under multiple BSs with our proposed improved NE strategy scheme, to further verify the superiority of our proposed strategy in the set context, we will cut the link between one of the previously set multiple BSs and the UAV, and implement the UAV and a single BS to construct a backhaul transmission link. Here we switch off the BS at (1000,1800) and all UAVs build a backhaul transmission link only with the BS at (1200,1200). The original direction of motion and speed of motion of the UAVs remain unchanged, and they continue to move away from the BS. At this point, we compare the average effective backhaul transmission rate and the small effective backhaul transmission rate obtained from the single BS link and the multi-BS link under both the improved NE strategy. The comparison results are shown in Figure 10.

As shown in the results of Figure 10, the average effective backhaul transmission rate R_{av} and the minimum effective backhaul transmission rate R_{min} both decrease as the UAV gradually moves away from the BS. The results of our proposed multi-BS link compared to the single BS link proposed in the paper by Liu et al. [33] are as follows. As shown in Figure 10 (a), the average effective backhaul rate R_{av} decreases due to the increasing distance between the UAV and the BS under both the UAV and single BS construction links and the multi-BS construction link, but the effect obtained is more obvious for the multi-BS link than for the single BS link, and the difference between the average effective backhaul rates of the two can reach a maximum of 1.7 Mbps and a minimum of 0.9 Mbps. This is because

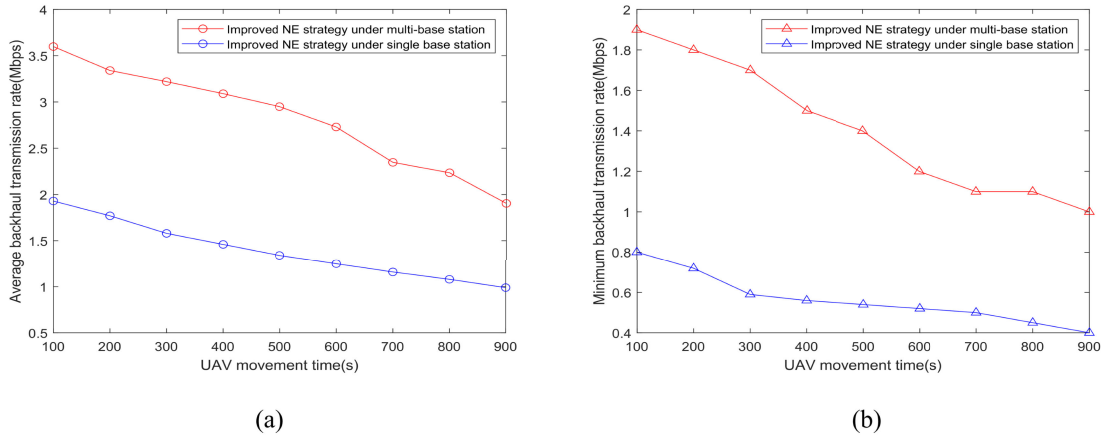


FIGURE 10. The average and minimum backhaul transmission rate of dynamic backhaul links with different number of BSs.

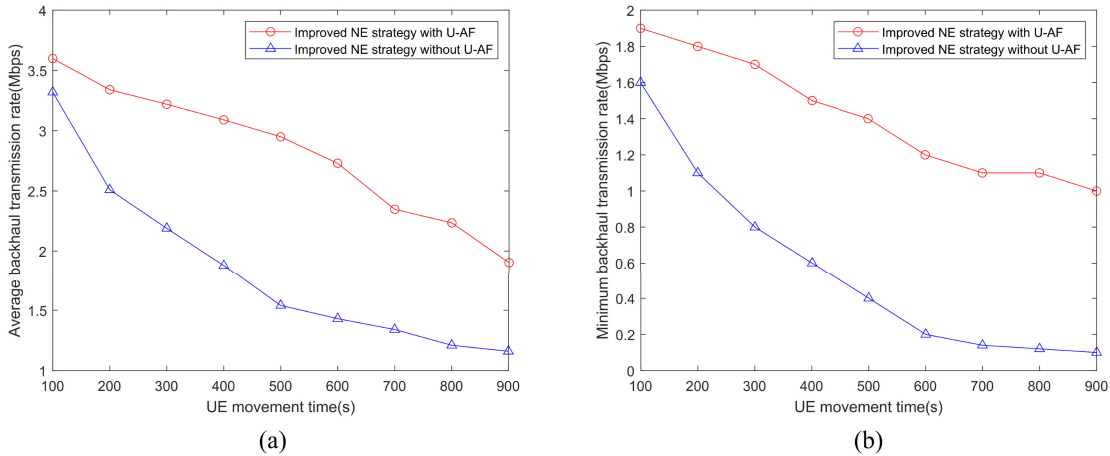


FIGURE 11. The average and minimum backhaul transmission rate of dynamic backhaul links with U-AF strategy or not.

our proposed strategy is more effective and applicable under multi-BS construction link. The minimum effective backhaul rate R_{\min} obtained in Figure 10 (b) is higher than the single BS link, with a minimum value of 0.3 Mbps. This makes our proposed enhanced NE strategy more effective in the multi-BS link, and further demonstrates the feasibility of our proposed scheme in a multi-BS context.

Liu et al. [33] use a purely random distribution of UAVs without incorporating any algorithms to implement UAV tracking of motion of UEs. To verify whether our proposed U-AF model has any effect on the results obtained by the improved NE algorithm, we compare the results obtained with and without the U-AF model, as shown in Figure 11. From Figure 11 (a) and (b), we can find that when the UE's movement time is within 100 s, the differences of R_{av} and R_{\min} between the two are small, only 0.28 Mbps and 0.3 Mbps, respectively. When the UE's movement time is 200 s and above, a significant gap appears between the results compared, and the maximum gap of R_{av} can reach 1.41 Mbps, while the maximum gap of R_{\min} can reach 1 Mbps. This

is because without the U-AF model, the UAV cannot track the UE in real time, and therefore cannot make reasonable updates to the UAV position. This reduces the user demand rate per UAV, which in turn affects R_{av} and R_{\min} . This demonstrates why the U-AF model and the improved NE algorithm are essential for achieving the maximum effective backhaul transmission rate, and also further validates the superiority of the U-AF model from the perspective of the improved NE algorithm.

V. CONCLUSION

This paper presents a network optimization scheme based on the anti-flocking and improved NE algorithm which optimizes the deployment of UAVs and realize the composition of multi-hop backhaul links, aiming to obtain the maximum service rate of UEs and the effective UAV backhaul transmission rate. The contribution of this paper is categorized into three main sections: 1) Predeploying UAVs in hotspots by applying the U-GWO algorithm; 2) Establishing a U-AF model to enable UAVs to track hotspot UEs in real time and

prevent UAVs to be too close; 3) Proposing an improved NE strategy to build backhaul links between UAVs and multi-BSs. The results show that the average service rate of UE with U-GWO algorithm is improved from 1 % to 5.77 % compared to other different swarm intelligence optimization algorithms. And the service rate obtained with U-AF algorithm is 43.2 % improved compared to the baseline scenario without U-AF algorithm. For UAV backhaul transmission link construction, the simulation results show that the proposed improved NE strategy improves the average effective backhaul rate by 12 %, the minimum backhaul rate by 84 % and the overall iteration number by 5 % on average compared to a pure NE strategy.

The algorithms in this paper are based on the premise that the UAVs are at the same altitude and the ground BS locations are randomly distributed. Since our proposed model is based on a set simulation context. But in practical application scenes, the situation to be considered is more complex, and it may reduce the performance of the algorithms proposed. Therefore, in future research, more factors of 3D space need to be added to investigate the UAV deployment tracking algorithm and UAV backhaul transmission link construction algorithm in 3D space more thoroughly. Specific elements that may need to be taken into account are also the size and complexity of the network, the availability of resources, and the dynamic nature of the network. In most practical cases, the environments of the backhaul transmission links we have constructed are relatively poor, and this will offset the relevance of our proposed scheme among some good backhaul environments. This also needs us to explore the relationship between positional migration and backhaul of UAVs in future studies. In terms of network resource utilisation, we need to artificially design the utility function. This also means that the process of designing a utility function requires a lot of effort and the utility function obtained, is not guaranteed to be efficient. Therefore we need more in-depth research on adaptive models of utility functions in the future.

REFERENCES

- [1] V. Sharma, M. Bennis, and R. Kumar, "UAV-assisted heterogeneous networks for capacity enhancement," *IEEE Commun. Lett.*, vol. 20, no. 6, pp. 1207–1210, Jun. 2016.
- [2] Z. Wei, M. Zhu, N. Zhang, L. Wang, Y. Zou, Z. Meng, H. Wu, and Z. Feng, "UAV-assisted data collection for Internet of Things: A survey," *IEEE Internet Things J.*, vol. 9, no. 17, pp. 15460–15483, Sep. 2022.
- [3] H. Ullah, N. G. Nair, A. Moore, C. Nugent, P. Muschamp, and M. Cuevas, "5G communication: An overview of vehicle-to-everything, drones, and healthcare use-cases," *IEEE Access*, vol. 7, pp. 37251–37268, 2019.
- [4] P. McEnroe, S. Wang, and M. Liyanage, "A survey on the convergence of edge computing and AI for UAVs: Opportunities and challenges," *IEEE Internet Things J.*, vol. 9, no. 17, pp. 15435–15459, Sep. 2022.
- [5] L. Wang, H. Zhang, S. Guo, and D. Yuan, "Deployment and association of multiple UAVs in UAV-assisted cellular networks with the knowledge of statistical user position," *IEEE Trans. Wireless Commun.*, vol. 21, no. 8, pp. 6553–6567, Aug. 2022.
- [6] Z. Na, C. Ji, B. Lin, and N. Zhang, "Joint optimization of trajectory and resource allocation in secure UAV relaying communications for Internet of Things," *IEEE Internet Things J.*, vol. 9, no. 17, pp. 16284–16296, Sep. 2022.
- [7] W. J. Yun, S. Park, J. Kim, M. Shin, S. Jung, D. A. Mohaisen, and J.-H. Kim, "Cooperative multiagent deep reinforcement learning for reliable surveillance via autonomous multi-UAV control," *IEEE Trans. Inf. Informat.*, vol. 18, no. 10, pp. 7086–7096, Oct. 2022.
- [8] J. Sabzehali, V. K. Shah, Q. Fan, B. Choudhury, L. Liu, and J. H. Reed, "Optimizing number, placement, and backhaul connectivity of multi-UAV networks," *IEEE Internet Things J.*, vol. 9, no. 21, pp. 21548–21560, Nov. 2022.
- [9] Y. Chen, W. Feng, and G. Zheng, "Optimum placement of UAV as relays," *IEEE Commun. Lett.*, vol. 22, no. 2, pp. 248–251, Feb. 2018.
- [10] M. Alzenad, A. El-Keyi, F. Lagum, and H. Yanikomeroglu, "3-D placement of an unmanned aerial vehicle base station (UAV-BS) for energy-efficient maximal coverage," *IEEE Wireless Commun. Lett.*, vol. 6, no. 4, pp. 434–437, Aug. 2017.
- [11] R. I. Bor-Yaliniz, A. El-Keyi, and H. Yanikomeroglu, "Efficient 3-D placement of an aerial base station in next generation cellular networks," in *Proc. IEEE Int. Conf. Commun. (ICC)*, May 2016, pp. 1–5.
- [12] C.-C. Lai, C.-T. Chen, and L.-C. Wang, "On-demand density-aware UAV base station 3D placement for arbitrarily distributed users with guaranteed data rates," *IEEE Wireless Commun. Lett.*, vol. 8, no. 3, pp. 913–916, Jun. 2019.
- [13] Z. Yuheng, Z. Liyan, and L. Chunpeng, "3-D deployment optimization of UAVs based on particle swarm algorithm," in *Proc. IEEE 19th Int. Conf. Commun. Technol. (ICCT)*, Oct. 2019, pp. 954–957.
- [14] A. Chowdhury and D. De, "RGSO-UAV: Reverse glowworm swarm optimization inspired UAV path-planning in a 3D dynamic environment," *Ad Hoc Netw.*, vol. 140, Mar. 2023, Art. no. 103068.
- [15] A. A. Saadi, A. Soukane, Y. Meraihi, A. B. Gabis, and A. Ramdane-Cherif, "A hybrid improved manta ray foraging optimization with Tabu search algorithm for solving the UAV placement problem in smart cities," *IEEE Access*, vol. 11, pp. 24315–24342, 2023.
- [16] J. Shi, P. Cong, L. Zhao, X. Wang, S. Wan, and M. Guizani, "A two-stage strategy for UAV-enabled wireless power transfer in unknown environments," *IEEE Trans. Mobile Comput.*, early access, Jan. 31, 2023, doi: 10.1109/TMC.2023.3240763.
- [17] O. S. Oubbati, A. Lakas, and M. Guizani, "Multiagent deep reinforcement learning for wireless-powered UAV networks," *IEEE Internet Things J.*, vol. 9, no. 17, pp. 16044–16059, Sep. 2022.
- [18] H. Mei, K. Yang, Q. Liu, and K. Wang, "3D-trajectory and phase-shift design for RIS-assisted UAV systems using deep reinforcement learning," *IEEE Trans. Veh. Technol.*, vol. 71, no. 3, pp. 3020–3029, Mar. 2022.
- [19] S. Fu, Y. Tang, N. Zhang, L. Zhao, S. Wu, and X. Jian, "Joint unmanned aerial vehicle (UAV) deployment and power control for Internet of Things networks," *IEEE Trans. Veh. Technol.*, vol. 69, no. 4, pp. 4367–4378, Apr. 2020.
- [20] S. Yang, D. Shi, Y. Peng, S. Yang, B. Zhang, and W. Yang, "Placement optimization for UAV-enabled wireless networks with multi-hop backhauls in urban environments," in *Proc. 21st ACM/IEEE Int. Conf. Inf. Process. Sensor Netw. (IPSN)*, May 2022, pp. 54–66.
- [21] Z. Li, X. Xia, and Y. Yan, "A novel semidefinite programming-based UAV 3D localization algorithm with gray wolf optimization," *Drones*, vol. 7, no. 2, p. 113, Feb. 2023.
- [22] J. Lyu, Y. Zeng, R. Zhang, and T. J. Lim, "Placement optimization of UAV-mounted mobile base stations," *IEEE Commun. Lett.*, vol. 21, no. 3, pp. 604–607, Mar. 2017.
- [23] S. Jiaqi, T. Li, Z. Hongtao, L. Xiaofeng, and X. Tianying, "Adaptive multi-UAV path planning method based on improved gray wolf algorithm," *Comput. Electr. Eng.*, vol. 104, Dec. 2022, Art. no. 108377.
- [24] M. Ye, Q.-L. Han, L. Ding, and S. Xu, "Distributed Nash equilibrium seeking in games with partial decision information: A survey," *Proc. IEEE*, vol. 111, no. 2, pp. 140–157, Feb. 2023.
- [25] Z. Lyu, G. Zhu, and J. Xu, "Joint maneuver and beamforming design for UAV-enabled integrated sensing and communication," *IEEE Trans. Wireless Commun.*, vol. 22, no. 4, pp. 2424–2440, Apr. 2023.
- [26] A. Al-Hourani, S. Kandeepan, and S. Lardner, "Optimal LAP altitude for maximum coverage," *IEEE Wireless Commun. Lett.*, vol. 3, no. 6, pp. 569–572, Dec. 2014.
- [27] S. Zhang, D. Wu, L. Jiang, X. Jin, and S. Cen, "Research on UAV access deployment algorithm based on improved virtual force model," *KSII Trans. Internet Inf. Syst.*, vol. 16, no. 8, pp. 1–21, 2022.
- [28] S. Mirjalili, S. M. Mirjalili, and A. Lewis, "Grey wolf optimizer," *Adv. Eng. Softw.*, vol. 69, pp. 46–61, Mar. 2014.

[29] G.-G. Wang, C.-L. Wei, Y. Wang, and W. Pedrycz, "Improving distributed anti-flocking algorithm for dynamic coverage of mobile wireless networks with obstacle avoidance," *Knowl.-Based Syst.*, vol. 225, Aug. 2021, Art. no. 107133.

[30] Y.-Q. Miao, A. Khamis, and M. S. Kamel, "Applying anti-flocking model in mobile surveillance systems," in *Proc. Int. Conf. Auto. Intell. Syst. (AIS)*, Jun. 2010, pp. 1–6.

[31] G. Bacci, S. Lasaulce, W. Saad, and L. Sanguinetti, "Game theory for networks: A tutorial on game-theoretic tools for emerging signal processing applications," *IEEE Signal Process. Mag.*, vol. 33, no. 1, pp. 94–119, Jan. 2016.

[32] N. Xing, Q. Zong, B. Tian, Q. Wang, and L. Dou, "Nash network formation among unmanned aerial vehicles," *Wireless Netw.*, vol. 26, no. 3, pp. 1781–1793, Apr. 2020.

[33] L. Liu, D. Wu, X. Jin, and S. Cen, "Backhaul transmission scheme for UAV based on improved Nash equilibrium strategy," *KSII Trans. Internet Inf. Syst.*, vol. 16, no. 8, pp. 2666–2687, 2022.



DUANPO WU received the B.S. degree from the College of Electronics and Information, Hangzhou Dianzi University, China, in 2009, and the Ph.D. degree from the College of Information Science and Electronic Engineering, Zhejiang University, China, in 2014. Since 2022, he has been an Associate Professor with Hangzhou Dianzi University. His research interests include intelligent signal processing, biological data analysis, and machine learning.



XINYU JIN has been a Professor with the Faculty of Information Science and Electrical Engineering, Zhejiang University, China, since 1999. His research interests include network communication and intelligent electronic systems.



TIANJUN WANG is currently pursuing the degree with Hangzhou Dianzi University, Hangzhou, China. His research interest includes wireless network communication.



SHUCHANG ZHANG is currently pursuing the degree with Hangzhou Dianzi University, Hangzhou, China. His research interest includes wireless network communication.



SHUWEI CEN is currently the Network Planning Supervisor of Hangzhou Branch of China Mobile Communications Group Zhejiang Company Ltd. He is mainly responsible for network planning and network specification.



LISHAN LIU is currently pursuing the degree with Hangzhou Dianzi University, Hangzhou, China. His research interest includes wireless network communication.



BING FAN received the B.S. degree in electric technology from the Huazhong University of Science and Technology, China, in 2000, and the M.S. degree in communication and information system from the Wuhan University of Technology, China, in 2003. Since 2019, she has been an Associate Researcher with Hangzhou Dianzi University. Her research interests include network communication, wireless sensor networks, laboratory construction, and management.

...